JOURNAL OF MATERIALS SCIENCE 29 (1994) 1441 – 1448

Determination of residual stresses in bimaterials

G. DREIER, G. ELSSNER, S. SCHMAUDER
Max-Planck-Institut für Metallforschung, Institut für Werkstoffwissenschaft, Seestraße 92, D-7000 Stuttgart 1, Germany

T. SUGA
Research Center for Advanced Science and Technology, University of Tokyo, Komaba 4-6-1, Meguro-ku, Tokyo 153, Japan

Residual stresses play a prominent role in the fracture process of bimaterials and therefore knowing these stresses prior to failure is important for understanding the mechanical behaviour of bimaterials. A critical assessment has been made of three methods for determining the residual stresses. These methods are: stress optical measurement, indentation method, and finite element method. With stress optical measurements the difference in the principal normal stresses, $\Delta\sigma$, can be determined. In the centre region adjacent to the interface, the measured stress values are in agreement with results from a simple analytical formula for the normal residual stresses parallel to the interface. Surface stresses at arbitrary locations can be obtained by the usual indentation technique. At the surface, stresses perpendicular to the interface are dominant and have the opposite sign to the stresses parallel to the interface. When there is no mechanical mismatch between the components the magnitude of the residual stresses can be estimated with the above-mentioned formula. Two-dimensional plane strain finite element calculations are in good agreement with the stress optical measurements.

1. Introduction

Metal/ceramic bimaterials offer superior properties over conventional alloys and have been widely studied because of their many potential applications [1]. Nevertheless, the use of bimaterials is limited by residual stresses which influence the failure characteristics of composites in general. Specifically, failure in these systems may initiate at the interface and propagate into the ceramic due to residual stresses even in the absence of an externally applied stress [2]. Therefore, calculation or measurement of residual stresses is an important issue in the development of strong metal/ceramic joints. Previously, the indentation technique has been used for obtaining a qualitative picture of residual stress states in metal/ceramic systems [3]. Nevertheless, quantitative analyses have not been performed for bimaterials.

The purpose of this study was to demonstrate that the principal features of residual stresses in bimaterials can be understood using simple methods such as stress optics or indentation techniques. To this end, we applied these techniques to a model glass/glass composite bimaterial to determine the non-singular residual stress fields near the interface. Results from these investigations will be discussed and compared with accompanying numerical studies using the finite element method (FEM).

We consider a bimaterial, designated materials 1 and 2, which is cooled by ΔT and which obeys the convention $\alpha_1 > \alpha_2$, according to Fig. 1, where α_1 and α_2 are thermal expansion coefficients. When displacements parallel to the interface are suppressed (e.g. at the centreline of the specimen, $x = 0$), the following expressions for the nominal residual stresses, σ^{res}, in materials 1 and 2 parallel to the interface are valid [4]

$$\sigma_{1x}^{res} = -1/2E^*\Delta\alpha\Delta T \quad (1a)$$

$$\sigma_{2x}^{res} = 1/2E^*\Delta\alpha\Delta T \quad (1b)$$

In the first equation, the difference in thermal expansion coefficients is obtained from Hooke's law as

$$\Delta\alpha = \begin{cases} (1+\nu_1)\alpha_1 - (1+\nu_2)\alpha_2 & \text{(plane strain)} \\ \alpha_1 - \alpha_2 & \text{(plane stress)} \end{cases} \quad (2)$$

and ν_1 and ν_2 are Poisson's ratios. In addition, the cooling interval, ΔT, is determined by the difference between room temperature, T_0, and the processing temperature, T_p

$$\Delta T = T_0 - T_p \quad (3)$$

and E^* is the mean Youngs' modulus of the bimaterial, defined as follows [5]

$$\frac{1}{E^*} = \frac{1}{2}\left(\frac{1}{E_1^+} + \frac{1}{E_2^+}\right) \quad (4)$$

In Equation 4, E_i^+ is given by

$$E_i^+ = \begin{cases} E_i/(1-\nu_i^2) & \text{(plane strain)} \\ E_i & \text{(plane stress)} \end{cases} \quad (5)$$

0022–2461

and E_i ($i = 1, 2$) are the Youngs' moduli of components 1 and 2.

Properties of the glass/glass bimaterials examined here are presented in Table I. Also shown are the amounts of nominal residual stresses, σ^{res}, according to Equation 1 for plane stress and plane strain, respectively. (The processing temperature of the glass/glass bimaterials under investigation is identical to the transition temperature of the glass with the lower transition temperature. Thus, typical cooling intervals, ΔT, are estimated to be about 400 °C.)

2. Experimental procedures

Bimaterials, according to Table I and with dimensions $l = 30$ mm, $w = 8$ mm, and $b = 4$ mm (Figs 1, 2), have been processed by diffusion bonding [6] and tested experimentally. With the bimaterial combinations given in Table I the elastic and thermal mismatch can be varied nearly independently.

2.1. Stress optical measurements

Isotropic materials such as glasses are ideal for optical stress investigation, because they become birefringent when mechanical stresses are present. Thus, the stress state of glass/glass bimaterials can be examined with stress optical methods under the polarization microscope, as shown schematically in Fig. 2.

The standard procedure for stress optical measurements is as follows. First, polarized light is transmitted through the bimaterial which contains residual stresses. Owing to these stresses, an optical path difference, Δs, results from the different propagation velocities between light waves which are oscillating in the direction of σ_1 and σ_2. In this situation the following relation with the stress state exists [7–10]

$$\Delta\sigma = \frac{\Delta s}{bk} \tag{6}$$

where $\Delta\sigma$ is the difference in principal normal stresses σ_1 and σ_2, Δs the optical path difference, k the stress optical coefficient, and b the specimen thickness. σ_1, σ_2, and σ_3 are the three principal normal stresses along the centre symmetry line of a bimaterial as shown in Fig. 2. When residual stresses are absent, no birefringency is observed and the specimen appears dark owing to the crossed setting of polarizer and analyser. This is shown in Fig. 3a for the bimaterial SF56/SF56; as expected, no thermal stresses are present after bonding, because the joined materials are identical. Conversely, when residual stresses are present, one can expect bright and dark regions as shown in Fig. 3b, which was taken from a BK7/CaNa (CaNa = sodium chloride glass) bimaterial. The dark areas are called isoclines and are regions of identical principal stress directions which are parallel to the polarizer and analyser settings, respectively. Because the polarizer was set parallel to the interface and the analyser was perpendicular to the interface, one principal stress direction, σ_1, is parallel to the interface, while the second one, σ_2, is perpendicular to the interface.

For quantification of the difference in the principal residual stresses $\Delta\sigma$, the optical path difference, Δs, in both adjoining glasses has been measured, once perpendicular to the interface at locations $x/w = 0$ and once parallel to the interface at $y/w = \pm 0.03$ (cf. Figs 1 and 2). All stress optical measurements were performed on a Zeiss microscope Axiophot equipped with a tilting compensator to ensure exact measurement of Δs. The bimaterial BK7/CaNa was examined first because the stress optical coefficient, k, of both these glasses was known and because these coefficients are nearly identical, as shown in Table II [11].

The characteristics of the stress difference, $\Delta\sigma$, along the symmetry line $x/w = 0$ of the bimaterial is shown in Fig. 4a. Near the interface, compressive stresses prevail in the material with the smaller thermal expansion coefficients (Sample 2 = BK7); conversely, tensile stresses dominate in the material with the larger thermal expansion coefficient (Sample 1 = CaNa). Another interesting feature is that the stress differences approach a maximum value at the interface and decrease with increasing distance from the interface passing through zero at $y/w \approx 0.25$. The magnitude of $\Delta\sigma$ at larger distances up to $y/w < 0.6$ is still non-vanishing.

Extrapolation of $\Delta\sigma$ to the interface yields a value of approximately 12 MPa, which is in good agreement with the plane strain nominal residual stresses, σ_x^{res}, as obtained from Equation 1 (cf, Table I). The optically measured values of $\Delta\sigma$ parallel to the interface are presented in Fig. 4b. The stresses do not vary appreciably along the interface except for the edge area. The variation of $\Delta\sigma$ is restricted to a narrow regime $0.35 < |x/w| < 0.5$ at the surface. This regime for x/w is in agreement with literature data obtained by FEM [12, 13]. The asymmetry of the stress difference, $\Delta\sigma$, in Fig. 4b is attributed to the interface flaw on the right-hand side of the bimaterial (cf. Fig. 3b).

TABLE I Material data [6] and amount of nominal residual stresses of the examined model composites

Bimaterial	E_1 (GPa)	ν_1	α_1 (10^{-6} K^{-1})	E_2 (GPa)	ν_2	α_2 (10^{-6} K^{-1})	$\lvert\sigma_x^{res}\rvert$ (MPa)	
							Plane strain	Plane stress
SF56/SF56	58	0.242	8.8	58	0.242	8.8	0.00	0.00
SF53/SF56	58	0.238	9.3	58	0.242	8.8	7.19	5.80
SF56/BaSF64	58	0.242	8.8	105	0.262	8.7	0.81	1.53
SF53/BaSF64	58	0.238	9.3	105	0.262	8.7	8.50	8.97
CaNa/BK7	70	0.240	8.6	81	0.208	8.3	12.99	5.80

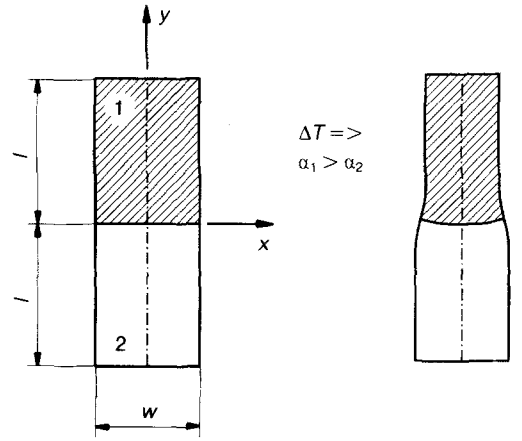

Figure 1 Schematic illustration of a bimaterial with coordinates and sign convention for thermal expansion coefficients before and after application of thermal stresses.

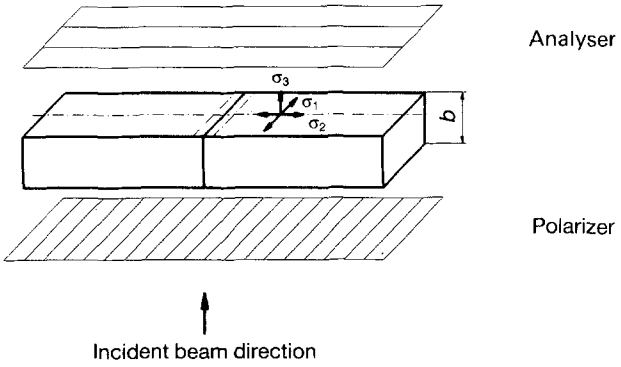

Figure 2 Schematic illustration of stress optical measurements with definition of principal stresses along the centre symmetry line ($x/w = 0$).

2.2. Indentation technique

The indentation method is based on the evaluation of the lengths of cracks emanating from the corners of Vickers indents. This method is widely used because it allows one to determine quickly the toughness values of brittle materials. Among several published evaluations, the method of Anstis *et al.* [14] has been shown to provide reliable results for glasses and ceramics. The following equation was derived for the stress intensity, K^E, caused by a Vickers hardness indentation [14] (Fig. 5)

$$K^E = 0.016(E/H)^{1/2}(P/c^{3/2}) \quad (7)$$

where E is the Youngs' modulus, H the Vickers' hardness, P the force of the indenting body, and $2c$ the diameter of the median crack. Equation 7 is based on empirical data and the fracture mechanical principle of crack growth due to an indenting body. One condition for determining the true toughness $K^E = K_{Ic}$ is a stress-free surface, because pre-existing surface stresses provide further loading on to the indentation cracks which may lead to crack propagation. However, this effect can be utilized to predict the magnitude of thermal residual stresses from the difference of indentation cracks in the presence of residual stresses when compared to the stress-free state. Under the assumption of linear elasticity, the true stress intensity

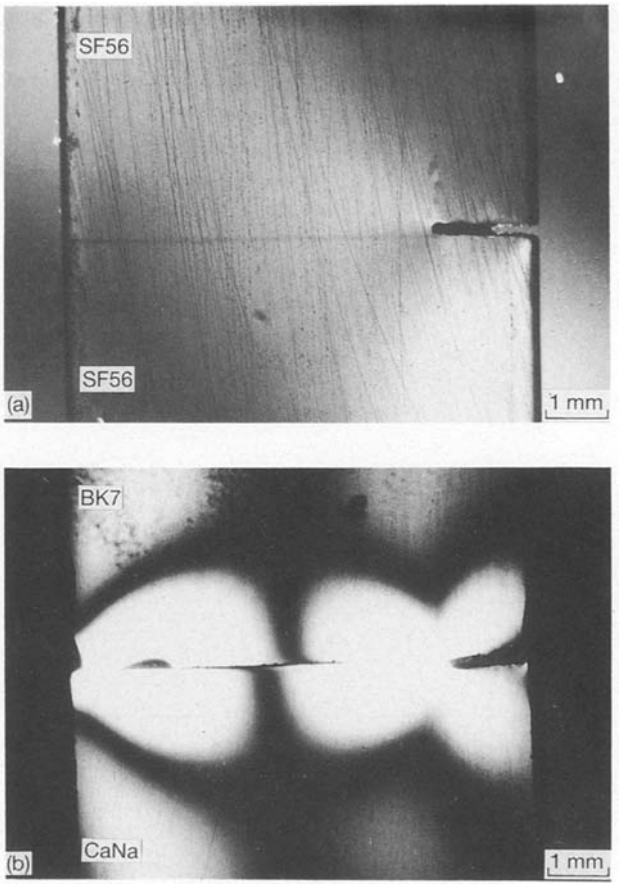

Figure 3 Light optical interference patterns for two bimaterials: (a) SF56/SF56 and (b) BK7/CaNa.

TABLE II Stress optical coefficient of examined materials for an optical wavelength $\lambda = 589.3$ nm

Glass	k (10^{-6} mm^2 N^{-1})
BK7	2.74
CaNa	2.75

is then a superposition of the indentation stress intensity, K^E, and of the residual stresses intensity, K^{res}. Under crack propagation conditions, the sum of both amounts to the critical stress intensity of the material, K_{Ic}

$$K = K^E + K^{res} = K_{Ic} \quad (8)$$

For this study we used the following relation between stress intensities due to residual stresses and lengths of surface cracks [15]

$$K^{res} = 2\sigma^r(c/\pi)^{1/2} \quad (9)$$

where σ^r is the unknown residual thermal stress component. These thermal stresses can be determined through analysis of Equations 7–9 when the toughness, K_{Ic}, of the material is known.

In the following discussion the thermal residual stress results are presented for tests conducted along the symmetry line $x/w = 0$ at the surface of a series of glass/glass bimaterials. The true toughness of each component was obtained using the same method with reference indents far away from the interface where

$\sigma^r = 0$. Measurements were performed in air at room temperature with an indentation force of $P = 9.81$ N for a 10 s duration. Crack lengths were measured immediately after unloading to eliminate influences from under critical crack growth due to atmospheric moisture.

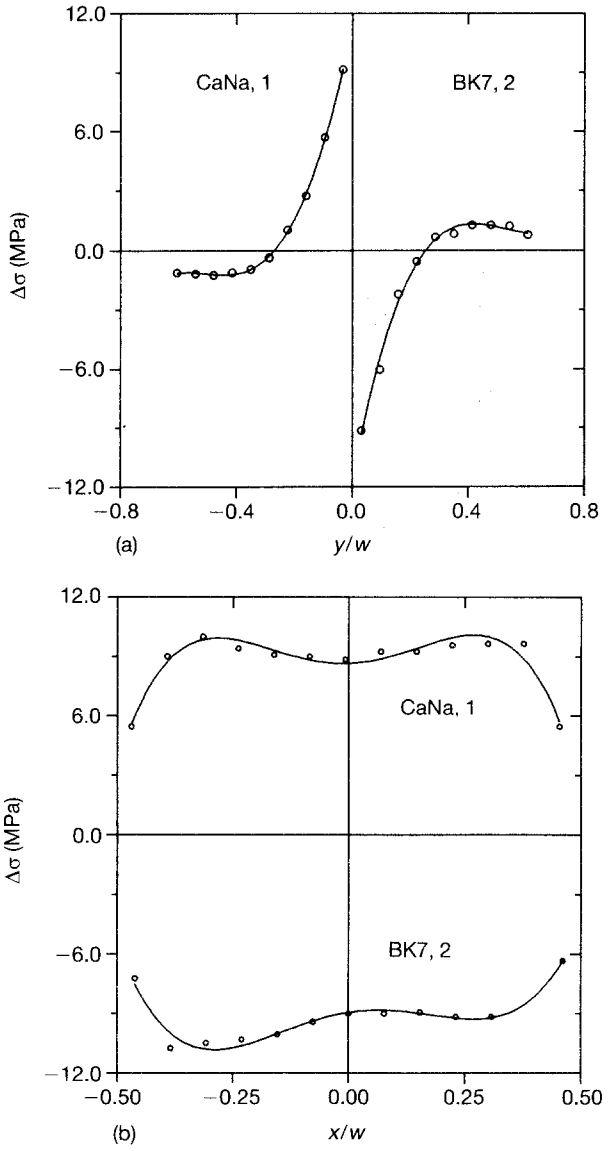

Figure 4 Difference of main principal stresses (a) perpendicular to the interface ($x/w = 0$), and (b) parallel to the interface for CaNa/BK7 as obtained from the light optical method ($y/w = \pm 0.03$).

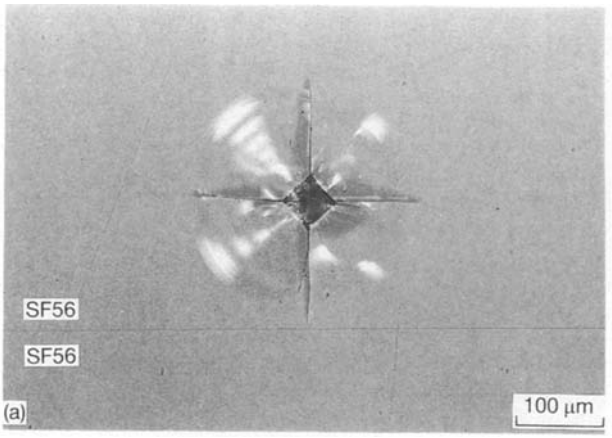

The effect of thermal residual stresses on growth of indentation cracks is clearly shown in Fig. 6a–c where Vickers hardness indentations were made into the materials at a distance of 130 μm ($y/w = 0.016$) away from the interface. In the system SF56/SF56, nearly all

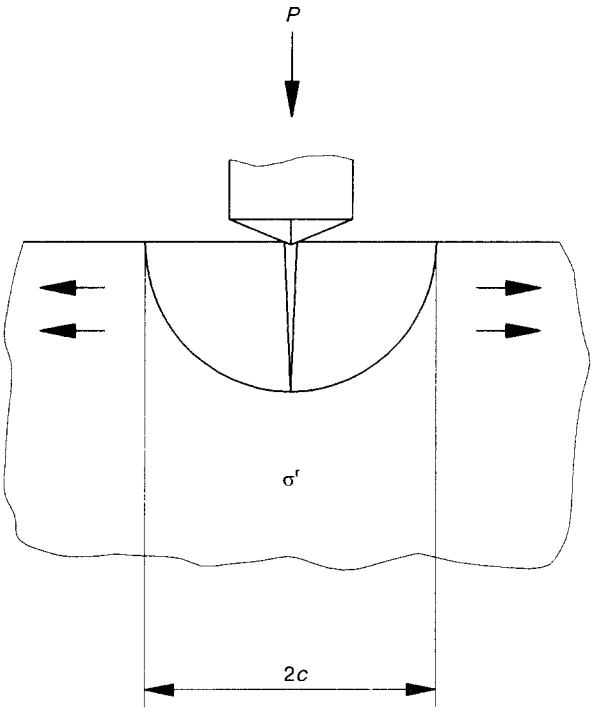

Figure 5 Schematic illustration of median crack system induced from Vickers indentation in a residually stressed body.

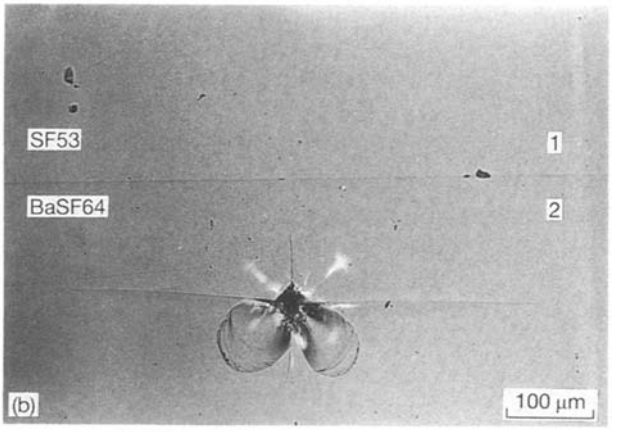

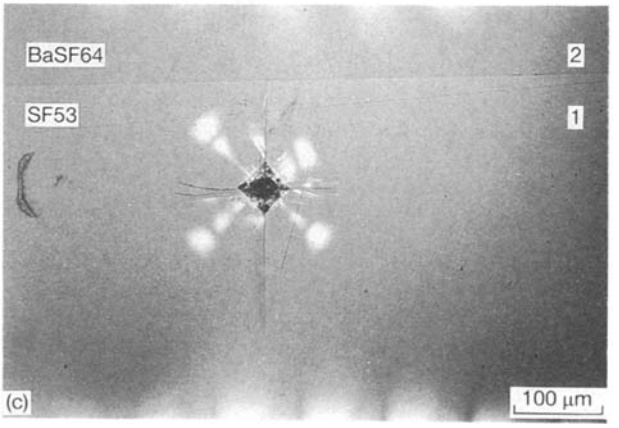

Figure 6 Typical crack patterns from indentation tests in the vicinity of glass/glass interfaces: (a) SF56/SF56, (b) on the BaSF64-side of SF53/BaSF64, and (c) on the SF53-side of BaSF64/SF53.

four cracks are identical and symmetric indicating the absence of residual stresses (Fig. 6a). Conversely, indents in the system SF53/BaSF64 behave quite differently. For example, in Fig. 6b, one can observe extremely elongated cracks parallel to the interface which indicate high tensile stresses ($\sigma^r_{2y} > 0$) perpendicular to the interface in BaSF64. In contrast, compressive stresses ($\sigma^r_{1y} < 0$) lead to a crack pattern with shorter cracks parallel to the interface in SF53, shown in Fig. 6c.

The length of cracks perpendicular to the interface are a measure of the thermal residual stresses parallel to the interface, σ^r_x. A comparison of Fig. 6b and c shows that tensile residual stresses are present in the material SF53 with the larger thermal expansion coefficient ($\sigma^r_{1x} > 0$) and balancing compressive stresses in the glass with the smaller thermal expansion coefficient ($\sigma^r_{2x} < 0$). By comparing the crack lengths parallel and perpendicular to the interface in either material, one can conclude that the effects of residual stresses perpendicular to the interface are dominant over those parallel to it, $|\sigma^r_y| > |\sigma^r_x|$.

Results obtained with the indentation method for stresses σ^r_y along the interface are shown in Fig 7a–d. According to continuum elasticity theory, residual stresses measured at the surface are expected to compare with a plane stress state rather than with plane strain. Fig. 7a and b contain the data for bimaterials without elastic mismatch, SF56/SF56 and SF53/SF56. The measured values for bimaterial SF56/SF56 are scattered around 0 MPa; therefore, this system is nearly free of residual stresses (Fig. 7a). In contrast, in the bimaterial SF53/SF56, compressive stresses ($\sigma^r_{1y} < 0$) are present in SF53 and tensile stresses ($\sigma^r_{2y} > 0$) in SF56, the glass with the smaller thermal expansion coefficient (Fig. 7b). This is an important observation, because it demonstrates that the thermal residual stresses, σ^r_y, measured at the surface are opposite in sign compared to stresses parallel to the interface, σ^r_x, which were obtained from the analytical expression in Equation 1. It is also interesting to note that the measured stresses are equal to the nominal residual stresses from Equation 1, $|\sigma^r_y| \approx |\sigma^{res}_x|$.

Results for the combination with elastic mismatch are shown in Fig. 7c and d. The system SF56/BaSF64, which is predicted to suffer a minimum of residual thermal stresses according to Equation 1 (Table I), is seen, in fact, to possess significant residual thermal stresses at the surface. Surprisingly, residual stresses reach values of about $\sigma^r_y \approx 7$ MPa which is approxim-

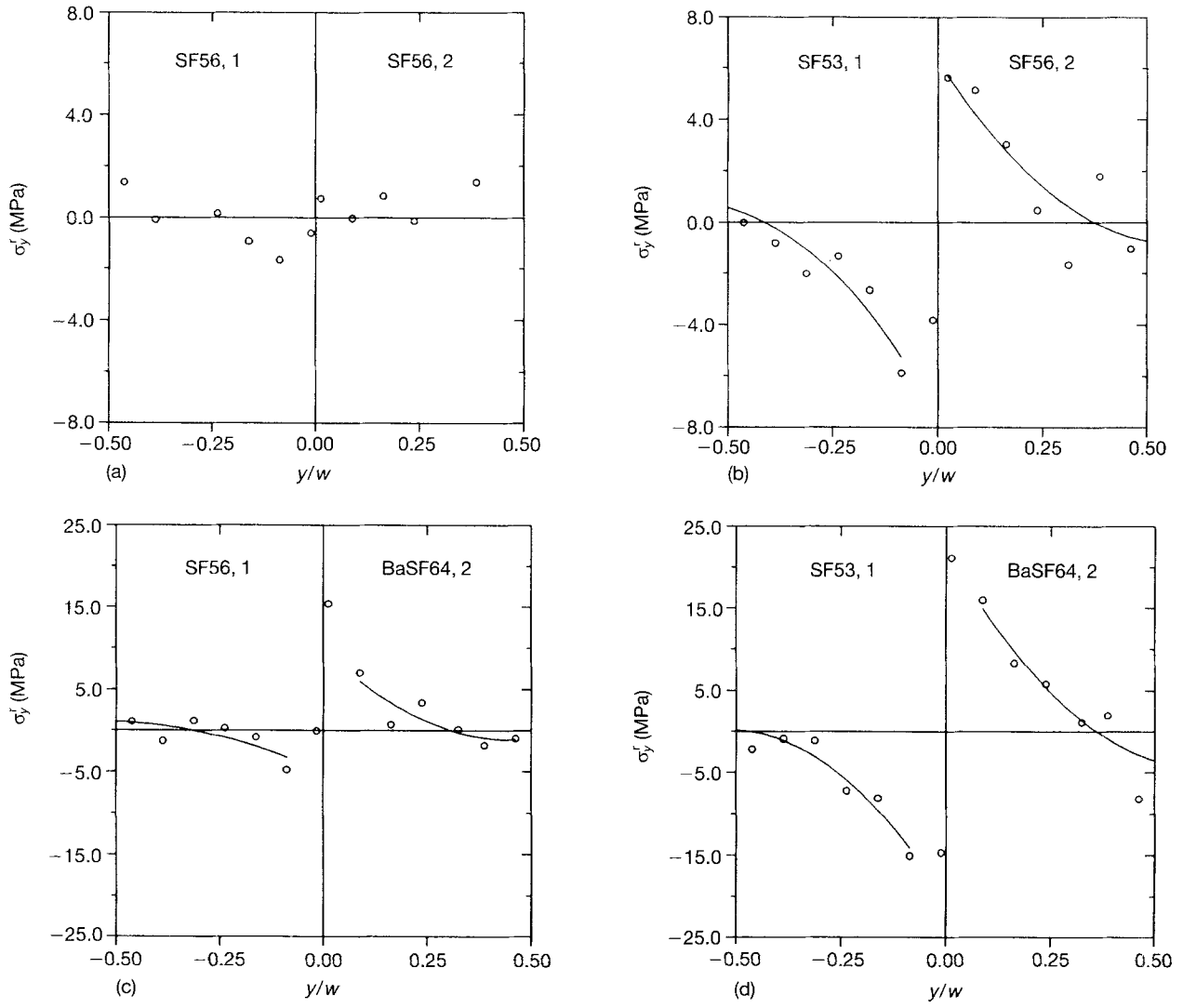

Figure 7 Residual stresses as obtained from the indentation technique along the centre symmetry line of a bimaterial ($x/w = 0$) in (a) SF56/SF56, and (b) SF53/SF56, (c) SF56/BaSF64, and (d) SF53/BaSF64.

ately four times the values predicted from Equation 1 for stresses parallel to the interface, σ_x^{res}.

Measured residual stresses, σ_y^r, in SF53/BaSF64 reach even higher values owing to a larger difference in thermal expansion coefficients in this bimaterial. Again, these measured residual stresses are well above those predicted from Equation 1 for stresses parallel to the interface. Hence, Equation 1 provides reasonable agreement with measured residual stress values σ_y^r only in the absence of elastic modulus mismatch.

3. Numerical analysis

Thermal residual stresses which develop during cooling were also examined by means of FEM. The bimaterial composite was modelled by an FE-mesh using eight-noded rectangular and six-noded triangular elements. Two-dimensional analyses based on plane strain and plane stress situations have been performed using the meshes shown in Fig. 8.

The normal and shear stresses parallel to the interface and under plane strain conditions at a distance $y/w = 0.025$ are shown in Fig. 9a for a CaNa/BK7 bimaterial. This distance was chosen according to the finite element mesh in the vicinity of the interface. The analysis predicts tensile stresses in the CaNa material which possesses the higher thermal expansion coefficient. By inspection of Fig. 9a one can observe that the normal stresses σ_y and σ_x are constant except for the near-edge regions; that is, the influence of the materials edge on the stresses is observable for $x/w > 0.35$. Parallel to the interface the calculation predicts stresses σ_x which are forty times the stresses σ_y.

The nature of stresses across the interface along the symmetry line $x = 0$ are shown in Fig. 9b. The stress component, σ_x, depicts the well-known discontinuity at the interface while the stress component, σ_y, is small compared to the σ_x stresses in the vicinity of the interface.

The principal normal stresses σ_1, σ_2, and σ_3 have also been calculated along the symmetry line assuming conditions of plane strain; these calculations were performed to simulate the stress optical measurements from Section 2.1. According to their orientation (σ_1 parallel to the interface, σ_2 perpendicular to the interface and σ_3 perpendicular to σ_1 and σ_2, cf. Fig. 2), σ_1 corresponds to σ_x and σ_2 to σ_y. The difference between principal stresses, $\sigma_1 - \sigma_2$, as a function of y/w is presented in Fig. 9c. These results agree closely with the results presented earlier in Fig. 4a. Thus, one may obtain the component σ_2 with stress optical measurements along the symmetry line because the stresses normal to the interface are vanishingly small compared to the stresses parallel to the interface ($\sigma_2 \gg \sigma_1$).

The nature of the differences of principal stresses parallel to the interface is shown in Fig. 9d. Again close proximity with measured stress characteristics is obtained, cf. Fig. 4b.

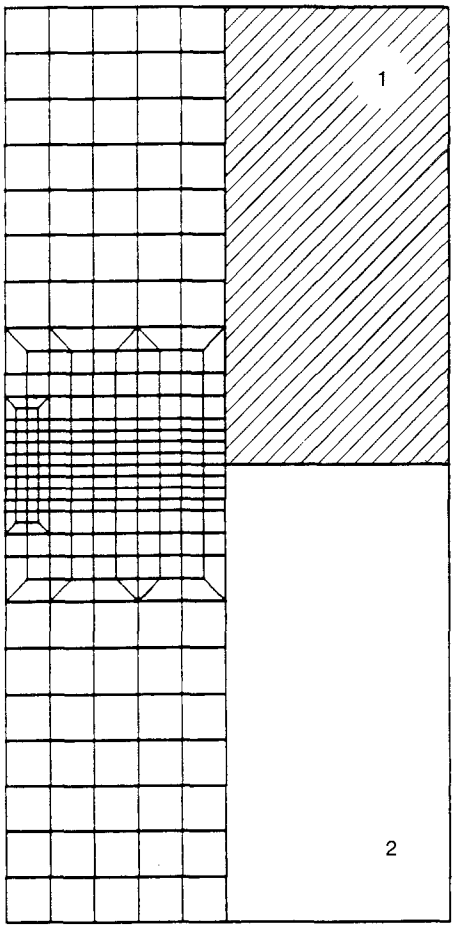

Figure 8 Finite element mesh of half a bimaterial specimen with mesh refinement along the interface.

4. Discussion

The comparison of residual stress results showed good agreement between stress optical and plane strain FE calculations for the bimaterials examined. The stresses parallel to the interface were predicted to be tensile in material 1 (with the larger thermal expansion coefficient); and compressive in material 2 (with the smaller thermal expansion coefficient), thus $\sigma_{1x} > 0$ and $\sigma_{2x} < 0$. The sign and magnitude of these stresses at the interface are in good agreement with predictions from the analytical solution of Equation 1 for the plane strain stresses at the interface in the center of the bimaterial, $1/2\ E^*\Delta\alpha\Delta T$.

Stresses perpendicular to the interface are expected to be comparatively small in plane strain and plane stress according to both stress optical measurements and the FEM calculations. This prediction, however, is not in agreement with results from surface measurements using the indentation technique. In addition, stress values determined from indentation methods were found to exceed greatly $1/2\ E^*\Delta\alpha\Delta T$ (Table I, Fig. 7d). This apparent contradiction between the three methods can be resolved when one considers that only surface stresses are obtained from the indentation technique while stress optical methods measure stresses through the full thickness of the bulk material. Thus, the stress information obtained via stress optics originates from the interior of the material; therefore, the assumption of a plane strain state is reasonable and provides the good agreement with plane strain FE calculations.

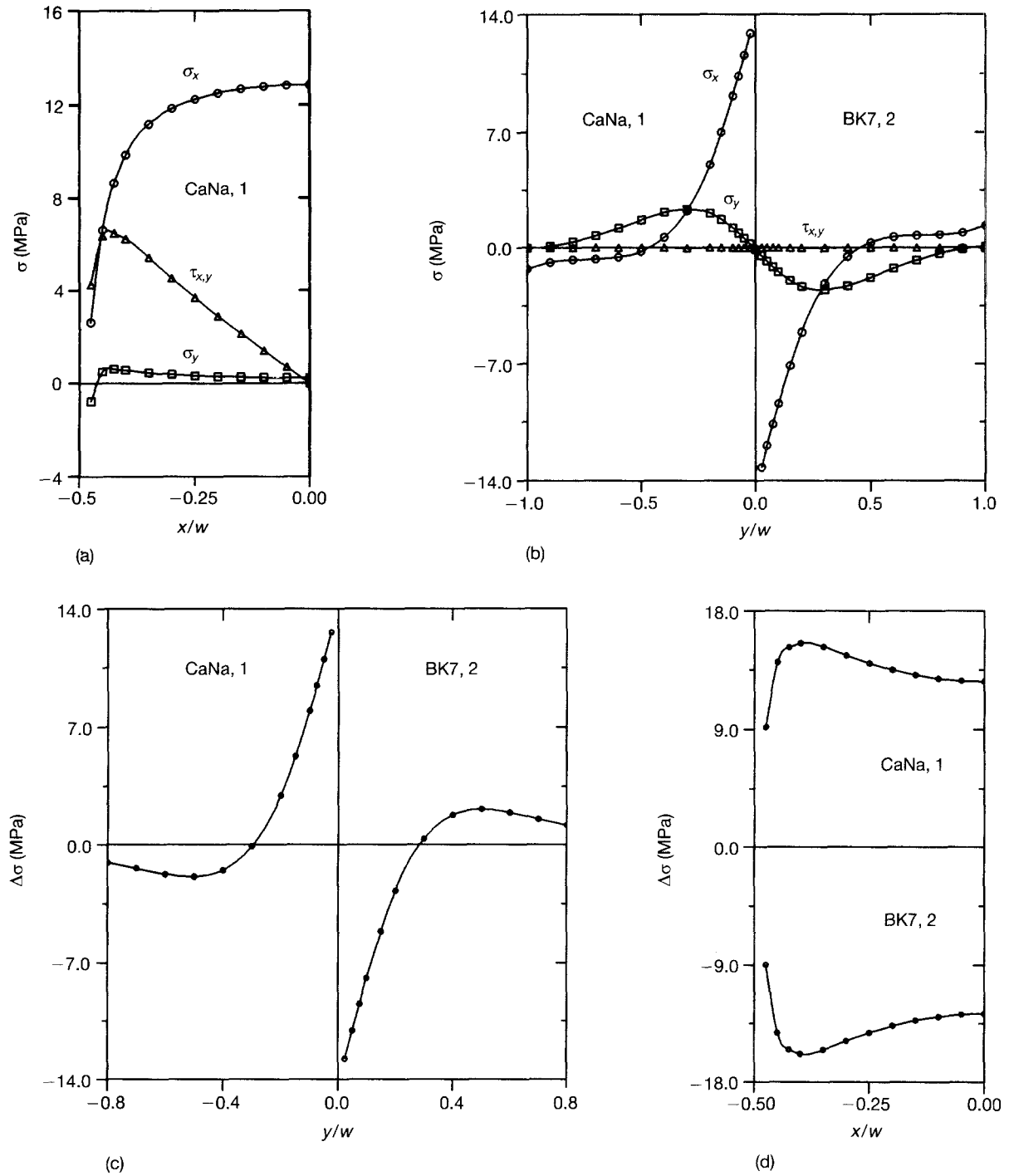

Figure 9 Residual stresses as obtained from plane strain finite element calculations in (a) CaNa parallel to the interface ($y/w = 0.025$) and (b) CaNa/BK7 along the centre line ($x/w = 0$) perpendicular to the interface and difference of main principal stresses (c) perpendicular to the interface ($x/w = 0$), and (d) parallel to the interface ($y/w = \pm 0.025$) for CaNa/BK7 as obtained from the finite element method under plane strain conditions.

In contrast to the plane strain results from stress optical measurements, the indentation technique provides insight into the stress state at the surface of the material. At the surface, high tensile stresses perpendicular to the interface ($\sigma^r_{2y} > 0$) dominate in the material which possesses the smaller expansion coefficient (material 2) and large compressive stresses ($\sigma^r_{1y} < 0$) are expected in material 1.

In the interior of the bimaterial, tensile stresses at the interface prevail in component 1 ($\sigma_{1x} > 0$, $\sigma_{1y} > 0$) while compressive stresses are found in material 2 with the smaller thermal expansion coefficient ($\sigma_{1x} < 0$, $\sigma_{1y} < 0$). Moreover, the stress component, σ^r_y, is small compared to the stress component parallel to the interface, σ^r_x. However, a full picture of the residual stress state in bimaterials will require more detailed numerical three-dimensional calculations.

5. Conclusion

It is well known that the strength of material joints is affected by the presence of thermal residual stresses, especially when a brittle component is joined with a compliant material of a larger thermal expansion coefficient. For example, this situation arises when a ceramic is bonded to a metal. In this case, residual stresses perpendicular to the interface are tensile in the material with the smaller thermal expansion

coefficient and can amount to stress levels in the ceramic well above the nominal stresses, as predicted by Equation 1. The purpose of this study was to evaluate three techniques which can be used to determine residual stresses in bimaterials.

The indentation technique is a simple and reliable method to obtain the non-singular part of these stresses. The stress state in the interior of the bimaterial along the symmetry line can be obtained through stress optical measurements. One can also use Equation 1 to determine the plane strain values in the vicinity of the interface.

For a more detailed view of singular stresses, the transition between the stress state in the surface and in the bulk as well as stress patterns near the interface, time-consuming finite element calculations, or other numerical methods, are necessary.

Acknowledgements

The research was supported by the Scientific Research Program of the Ministry of Monbusho for Joint Research between the University of Tokyo and the Max-Planck-Institut für Metallforschung under Grant 02044039 and by the German Research Foundation (DFG project El 53/13-1); the support is gratefully acknowledged. Optical glasses for the experiments were supplied by SCHOTT and Company, Mainz, and is gratefully acknowledged. The authors thank Dr Steve Rozeveld for valuable suggestions in improving the manuscript.

References

1. G. ELSSNER, T. SUGA and M. TURWITT, *J. de Phys.* **46** (1985) C4-597.
2. K. SUGANUMA, T. OKAMOTO, M. KOIZUMI and M. SHIMADA, *J. Mater. Sci. Lett.* **4** (1985) 648.
3. A. G. EVANS, M. RÜHLE and M. TURWITT, *J. de Phys.* **46** (1985) C4-657.
4. K. MIZUNO, K. MIYAZAWA and T. SUGA, *J. Faculty Eng. Univ. Tokyo* **39B** (1988) 401.
5. D. R. MULVILLE, P. W. MAST and R. N. VAISHNAV, *Eng. Fract. Mech.* **8** (1976) 555.
6. G. DREIER, M. MEYER, S. SCHMAUDER and G. ELSSNER, *Acta Metall. Mater.* (1991) in press.
7. K. FINK and C. ROHRBACH, "Handbuch der Spannungs- und Dehnungsmessung" (VDI, Düsseldorf, 1978) p. 220.
8. H. WOLF, "Spannungsoptik" (Springer, Berlin 1961) p. 582.
9. A. KUSKE, "Taschenbuch der Spannungsoptik" (Wissenschaftliche Verlagsgesellschaft, Stuttgart, 1971) p. 513.
10. N. N., "Bestimmung der Spannungen in Verschmelzungen von Glas mit Glas", DIN 52327, Teil 1 (1977).
11. MARC CLEMENT, Schott glass company, private communication (1991).
12. S. SCHMAUDER, in "Acta Scripta Metallurgica Proceedings Series 4," edited by M. Rühle, A. G. Evans, M. F. Ashby, J. P. Hirth (Pergamon Press, Oxford, 1990) p. 413.
13. A. G. EVANS, M. C. LU, S. SCHMAUDER and M. RÜHLE, *Acta Metall.* **34** (1986) 1634.
14. G. R. ANSTIS, P. CHANTIKUL, B. R. LAWN and D. B. MARSHALL, *J. Am. Ceram. Soc.* **64** (1981) 533.
15. J. C. NEWMAN and I. S. RAJU, *Eng. Fract. Mech.* **15** (1981) 185.

Received 6 April 1992
and accepted 8 July 1993